8th International Symposium on Friction Stir Welding
MARITIM Seehotel Timmendorfer Strand, Germany

The Influence of Friction Stir Weld Tool Form and Welding Parameters on Weld Structure and Properties: Nugget Bulge in Self-Reacting Friction Stir Welds

Author Details:

Surname	Schneider	First name	Judy
Company	Mississippi State University		
Address	Mechanical Engineering Department		
		Town	Mississippi State
Postcode	MS 39762	Country	USA
Telephone	662-325-9154	Email	schneider@me.msstate.edu

Co-author (1):

Surname	Nunes	First name	Arthur
Company	NASA MSFC		
Town	Marshall Space Flight Center	Country	USA
Telephone	256-544-2699	Email	Arthur.c.nunes@nasa.gov

Co-author (2):

Surname	Brendel	First name	Michael
Company	University of Illinois		
Town	Urbana-Champaign	Country	USA
Telephone	256 961-0032	Email	brendel2@illinois.edu

SYNOPSIS (~500 words)

The Influence of Friction Stir Weld Tool Form and Welding Parameters on Weld Structure and Properties: Nugget Bulge in Self-Reacting Friction Stir Welds

J.A. Schneider[1], A.C. Nunes, Jr[2]., and M.S. Brendel[3]
[1] Mississippi State University
[2] NASA Marshall Space Flight Center
[3] University of Illinois at Urbana-Champaign

Although friction stir welding (FSW) was patented in 1991, process development has been based upon trial and error and the literature still exhibits little understanding of the mechanisms determining weld structure and properties. New concepts emerging from a better understanding of these mechanisms enhance the ability of FSW engineers to think about the FSW process in new ways and must inevitably lead to advances in the technology.

A kinematic approach in which the FSW flow process is decomposed into several simple flow components, a translation, a rotation of a plug of metal adjacent to the tool, and a ring vortex flow component surrounding the tool, has been found to explain the basic structural features of FSW welds and to relate them to tool geometry and welding parameters.

Recently this kinematic concept has been applied to the "self reacting" (SR)-FSW process (See Figs. 1 and 2), in which the weld metal is grasped between shoulders attached to and rotating with the weld tool and does not require a heavy supporting anvil to balance a plunge load applied from one side only as in the "conventional" (C)-FSW process.

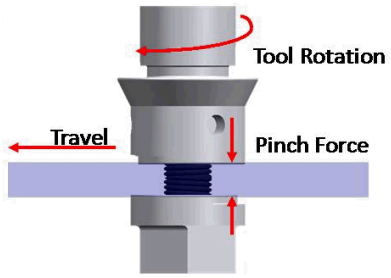

Figure 1. Tool geometry for a SR FSW tool.

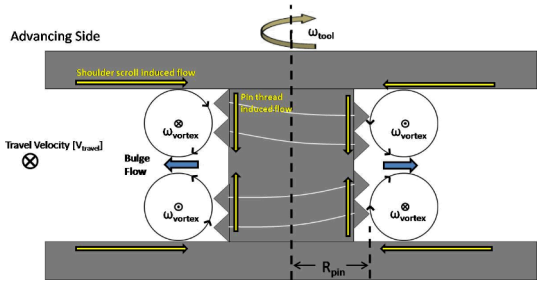

Figure 2. Basic material flow model.

A correlation between the lateral bulging of the nugget, the grain-refined region in the weld center, and the strength of the weld was found in a set of empirical SR-FSW data. Nugget material is generated by the very high shear deformation rate imposed on the weld metal as it is engulfed by and abandoned by the rotating plug of metal adjacent to the tool. The central bulge is a distortion of the nugget caused by the ring vortex flow component (See Fig. 2). A very rough estimate of the extent of bulge can be computed in terms of weld parameters and certain geometric features of the SR-FSW tool.

Because of the correlation of bulge with strength, the bulge computation relates weld parameters and tool geometry to weld strength. This correlation presents a way to select parameters and geometry so as to optimize weld strength. It also provides clues that may ultimately explain why the weld strength varies within the sample population.

The Influence of Friction Stir Weld Tool Form and Welding Parameters on Weld Structure and Properties: Nugget Bulge in Self-Reacting Friction Stir Welds

J.A. Schneider, Mississippi State University, Mississippi State, USA

A.C. Nunes, Jr., NASA, Marshall Space Flight Center, USA

M.S. Brendel, University of Illinois, Urbana-Champaign, USA

SYNOPSIS

Although friction stir welding (FSW) was patented in 1991 [1], process development has been based upon trial and error and the literature still exhibits little understanding of the mechanisms determining weld structure and properties. New concepts emerging from a better understanding of these mechanisms enhance the ability of FSW engineers to think about the FSW process in new ways, inevitably leading to advances in the technology.

A kinematic approach in which the FSW flow process is decomposed into several simple flow components has been found to explain the basic structural features of FSW welds and to relate them to tool geometry and process parameters [2, 3]. Using this modelling approach, this study reports on a correlation between the features of the weld nugget, process parameters, weld tool geometry, and weld strength. This correlation presents a way to select process parameters for a given tool geometry so as to optimize weld strength. It also provides clues that may ultimately explain why the weld strength varies within the sample population.

INTRODUCTION

Development of friction stir welding parameters has relied on a "trial and error" approach toward establishing process parameters and weld tool design. Process parameter ranges are typically established by FSWing over a range of RPM and travel speeds in fixed displacement control mode, allowing the load to vary as needed. Most reported studies do not consider or provide sufficient details of the weld tool for assessing possible relationships between the process parameters and the tool geometry. Tensile tests and microstructures are analyzed to distinguish "good" from "bad" welds. The basis for determining "bad" welds is either low tensile property data or structural defects. Several studies have been published which attempt to relate process parameters, typically through torque [4], or energy [5-7] applied to the weld, with "good welds".

Defects generally comprise internal voids, joint line remnants, and root flaws. Generic process maps have been developed which suggest that not all weld defects result from a single source outside of a "good parameter" envelope [8. 9]. Trends have been reported in the literature in which defects are reduced with increasing travel speed for a given tool design [10, 11]. Although opposite trends between welding speed and defect formation have been reported to occur among different aluminium alloys [11].

The weld temperature has been reported to be chiefly dependent on the tool rotation speed [12]. At higher tool rotations, more material is reported to be involved in the nugget formation which is attributed to hotter temperatures promoting a wider area of plasticized material flow [13]. A pseudo heat index (PHI) has been proposed to quantify the heat input level required to eliminate defects [14, 15]. However, other studies have reported holding this index constant does not produce welds of similar quality [16].

Attempts to relate tool geometry to weld quality have focused on smooth, threaded, or tapered pin tool surfaces, with or without flats [17-28]. No consistency has been reported in the literature regarding trends in the formation of defects associated with tool geometry other than that use of threads on the pin tool appear to mitigate the formation of defects [17, 23, 27]. Most of these studies have used a threaded pin with a smooth shoulder [17-28]. Threads on the pin tool have also been credited with promoting a vortex motion which stabilizes the rotational zone which reduces voids or lack of fusion [17, 23, 27]. Coarser pitch pins are reported to promote a larger working volume or volume of material influenced by the action of the pin tool [24].

Several researchers have distinguished between shoulder-flow- induced and pin-flow - induced flow defects [29-33]. If the defect occurs on the advancing side (AS), it is reported to be related to insufficient shoulder flow to fill a cavity left in the wake of the weld [29, 30]. The shoulders in these studies are assumed to be smooth due to the reported use of a lead angle on the tool. Several studies which use scrolled shoulders note similar defects although they attribute the defect to inadequate plunge load [33].

BODY OF PAPER

Process Modeling

A kinematic model [2] will prove useful in interpreting the experimental data obtained in this study. This approach conceives of a rotating plug of metal attached to the weld tool and translated along the weld seam with the tool. The rotating plug of metal is bounded by the tool surface and a shearing surface, observed to be very thin, separating the rotating plug from the fixed body of weld metal outside the plug. Figure 1 illustrates the metal flow crossing this boundary which is exposed to a very high shear strain rate ($\dot{\gamma}$) given in equation 1 that is dependent on the pin radius (R), tool rotation (ω) and shear zone thickness (δ). Typical strain rates predicted in the range of 10^3 to 10^5 s^{-1} approach those of ballistic conditions in which like grain refinement has been reported [34, 35]. . As the rotating plug moves along the weld seam, it entrains elements of metal, rotates them, and abandons them in the wake of the weld tool.

$$= \frac{R*\omega}{\delta} \qquad \text{[eqn. 1]}$$

$$\gamma = \frac{R*\omega}{V} \qquad \text{[eqn. 2]}$$

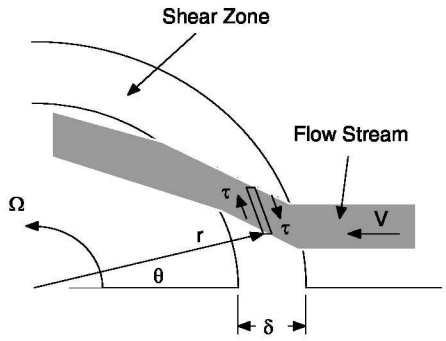

Figure 1. Metal entering severe shear zone surrounding tool.

The increment of shear strain (γ) the metal experiences as it enters the severe shear zone can be approximated using equation 2 where V is the tool travel velocity. At the reported temperatures range of 0.8-0.9 times the solidus melting temperature (T_{mp}) of the alloy, the flow stress of the metal is almost uniform in the close vicinity of the tool and shear surface [36]. Because the metal flow stress depends mostly on temperature, only minor variations in the flow stress are also expected close to the tool.

The weld tool typically has a threaded pin which creates a ring vortex velocity field with pronounced axial as well as radial flow velocity. This axial field component is responsible for retaining metal within the rotating plug during multiple revolutions as reported in other studies where markers have traced out metal paths rotating multiple times around the weld tool [37]. The ring vortex flow field adds perturbations of its own to the weld macrostructure. The kinematic model relates weld parameters and tool geometry to weld structure and offers ways to control weld structure to eliminate defects.

This kinematic concept has been applied to the both the conventional (C)-FSW and self reacting (SR)-FSW process as illustrated in Figure 2. The C-FSWing process reacts the forces generated by the tool against a backing anvil whereas the SR-FSW process grasps the metal between shoulders attached to and rotating with the weld tool to eliminate the need for the supporting anvil. The SR-FSW process is modeled as two mirrored, back-to-back C-FSW processes.

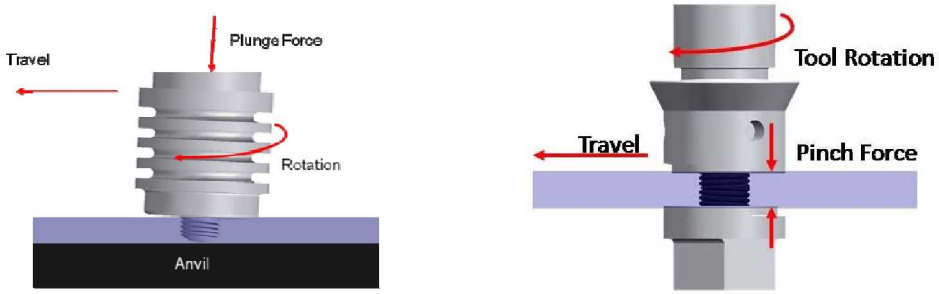

Figure 2. Comparison of conventional (C)-FSW process (a) versus the self-reacting (SR)-FSW process (b). Note the absence of the backing anvil in the SR-FSW process.

Experimental Procedure

The SR-FSWed butt welds in this study were made in 0.357" thick panels of 24" long AA2195-T87 panels. Table I summarizes the range of process parameters evaluated at constant pinch force. A single scrolled shoulder was used on the root and crown sides with a 1.2" in diameter and an inward inverse thread pitch of 0.12". A left hand (LH)/right hand (RH) threaded tool pin was used with a 0.5" in diameter and inverse thread pitch of 0.07". The LH/RH configuration served to push material toward the center of the workpiece plate thickness.

Table I. Summary of SR-FSWing process parameters.

Specimen ID	Process pitch (rev/in)
A1	9.1
A1	13.6
A3	18.2
E1	22.7
E2	27.3
E3	31.8
B1	7.1
B2	10.7
G1	12.5
B3	14.3
G2	16.1

Representative transverse cross sections were prepared from each weld panel using standard metallographical processing. A Keller's etch was used to reveal the macrostructure.

Standard 1" wide tensile bars were prepared and tested in room temperature, uni-axial tests conducted perpendicular to the welding direction. The tensile tests were run in accordance with ASTM standard E8 [38].

Results and Discussion

Figure 3 shows three representative transverse sections from the SR-FSW specimens in this study with pronouncedly different nugget shapes. The profile of the weld nugget in Figure 3a shows an hour-glass shape with a width that extends from roughly the pin diameter at the mid-plate to almost the shoulder width (more accurately the width of attachment of the weld metal to the shoulder) at the root and crown surfaces. In Figure 3b the nugget edges "flatten" along the pin center as the heat affected zone (HAZ) moves radially out away from the nugget. In Figure 3c a radial bulge emerges in the previously flattened nugget edge at the pin center.

Although the nugget geometry displays a similar profile on the AS advancing side (AS) and retreating side (RS), this study focuses on the changes to the AS profile since the sharp demarcation between the nugget and the TMAZ makes it easier to resolve.

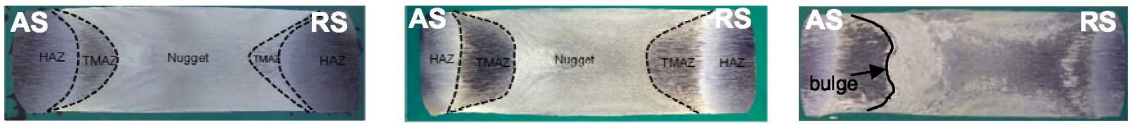

(a) B1 (b) G1 (c) G2

Figure 3. A variation in SR-FSW nugget as the tool rotation is increased. A pronounced change can be observed in the TMAZ/nugget boundary on the AS with the emergence of a nugget bulge in (c).

Overlay traces of the AS profile are summarized in Figure 4 for transverse sections of a series of SR-FSWs made with increasing tool rotation speed at constant travel and pinch

force. In Figure 4 the same kind of profile development is shown with increasing tool rotation speed as was observed in Figure 3. The initial hour-glass parabola flattens around the pin center prior to the emergence of a nugget bulge. Visual inspection of the nugget bulges often reveal the presence of voids, which are correlated with low tensile strength.

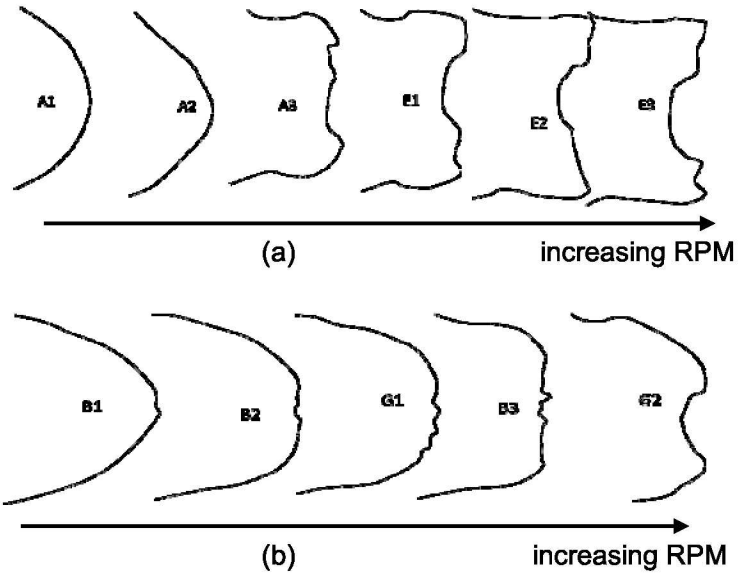

Figure 4. Variation in AS profile at 11 ipm (a) and 14 ipm (b) as a function of increasing tool rotation. As the tool rotation increases so does the extent of the central nugget bulge.

To correlate weld strength with the changes to the nugget profile, tensile tests were conducted using 3 samples per weld panel. The ultimate tensile strength (UTS) is averaged and plotted in Figure 5 versus tool rotation speed for each of the two travel speeds investigated. Commensurate with the change in AS profile is a corresponding drop off in UTS values.

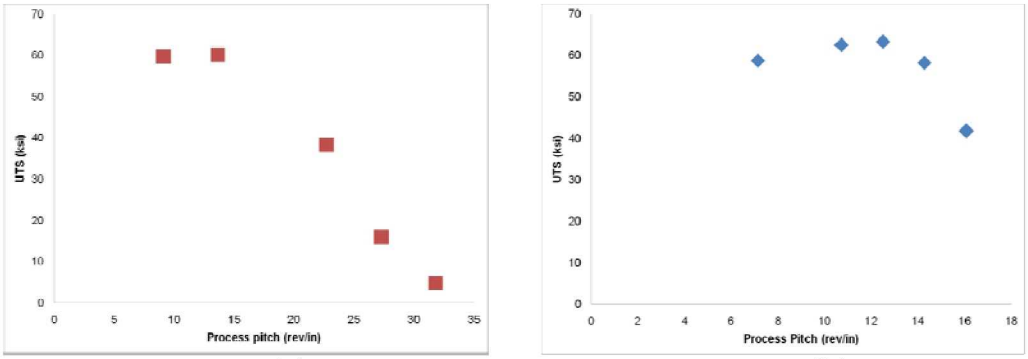

Figure 5. As the nugget bulge develops, a corresponding drop off in UTS (ksi) is observed at the travel speeds investigated: (a) 11 ipm, and (b) 14 ipm.

The velocity field components of the kinematic model of metal flow in the vicinity of the FSW tool explain the observed changes in nugget geometry with changes in spindle speed and weld speed. The velocity field components (with respect to the tool) include a transverse velocity field equal and opposite to the tool travel velocity, a rotation inside the shear surface equal to the tool rotation, and a ring vortex field with both axial and radial velocity components surrounding the tool. The ring vortex field is driven by both the pin threads and the scroll on the shoulder. A scrolled shoulder pushes the weld metal radially toward the tool center-line, and the pin threads force weld metal axially down the pin away the shoulder toward the weld metal central plane as illustrated in Figure 6. At the central plane the opposing axial flows from the two shoulders meet and force a radial outflow of metal at the central plane. Refined nugget metal is carried along by this radial flow during the time interval when the ring vortex flow is still active after the nugget metal exits from the rotating plug to form a nugget bulge at the central plane of the weld metal. The resulting increase in the nugget width is in agreement with observations of other researchers of an increase in nugget region attributed to the hotter welds resulting from the spindle speeds [13]. This is not just an increase of the amount of plasticized material involved in the FSW process, but an indication of a radial flow increment induced by tool threads or shoulder scrolls. Other researchers also report void formation in the region where ring vortex velocity fields interact [29, 30, 33].

In order to connect nugget bulge to weld parameters, the driving mechanism for the ring vortex circulation must be considered. It is assumed that the peripheral velocity of the ring vortex field is imposed by either the radial velocity of metal imposed by the shoulder scroll or the axial velocity imposed by the pin threads or by their joint action. For present purposes the coarser pitch, pin thread or shoulder scroll will be assumed dominant. Given a ring vortex circulation rate, the bulge increment depends upon how long the circulation is active for a given weld cross section. Supposing that the circulation is active for a given and roughly constant distance behind the tool, the time this distance is covered is inversely proportional to the tool's travel velocity along the weld. On this basis an approximate relation between nugget bulge and tool geometry and process parameters can be constructed. This relation is presented in equation 3, where Δ is the nugget bulge, R is the tool pin radius, ω is the tool rotation, P is the inverse pitch of the coarser thread, and V is the travel velocity along the weld seam. Precise computations are not to be expected from the relation, but, given the correctness of the assumptions, it should yield trends.

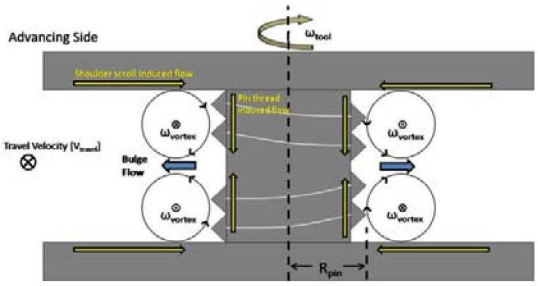

Figure 6. Basic material flow model in SR-FSW.

$$\Delta = \frac{R}{2}\left(1 - \cos\left(\frac{P}{V} * \frac{\omega}{\pi}\right)\right) \qquad \text{[eqn. 3]}$$

Figure 7 shows the macrostructure of a weld exhibiting reduced strength. The hour-glass nugget shape described in Figure 3 has transformed to a simple cylinder with a mid-plane bulge in Figure 7a if a very thin layer of nugget material following the shoulder contact area is ignored. Outside the nugget the coarse pancake-like parent metal grains (shaped by the rolling process that formed the plate) appear to be displaced upward and outward near the

bulge and upward, then downward near the shoulder in the vortex circulation described above with the kinematic flow model of the FSW process. Within the bulge region (Figure 7b), banding can be observed, typical of nugget material observed in conventional FSWs.

The edge of the nugget region traces out the residue of the shear surface as distorted by subsequent vortex flow. A span of nugget material between shoulder surface and shear surface implies that the weld metal is sticking to the shoulder and shearing beyond it within the weld metal. The minimal thickness observed in Figure 7a for the span of nugget material between shoulder surface and shear surface could be a result of slippage at the shoulder surface with a layer of disturbed metal masquerading as a thin span of nugget material. It could also be a result of the sweeping away of the thicker parts of a nugget material span by the ring vortex circulation. A little hump of apparent nugget material rising from the shoulder surface at the bottom left of Figure 7a and an arguable, barely perceptible hump descending from the upper shoulder surface favor the "sweeping away" concept with the implication of sticking at the shoulder surface.

Within the nugget material adjacent to the bulge region are areas containing multiple voids as shown in Figure 7c. The details of the mechanism by which these voids form is under study, but is not yet understood. It is known that material on the weld metal surface can be ingested deep into the weld; voids might be entrained into the weld by the ring vortex circulation. It is known that velocity gradients can produce tensile stresses which, for example, can produce central bursts in extrusions; voids might be produced by velocity gradients in the metal flow field near the nugget.

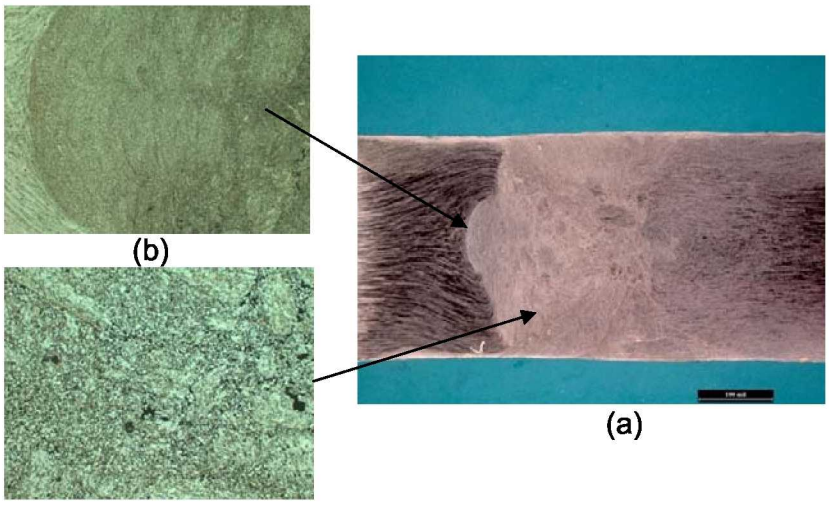

Figure 7. Image of E2 (a) showing close-up of nugget bulge (b) and associated voids in adjacent region (c).

Figure 5 shows a slight increase in UTS with increased spindle speed prior to a precipitous drop. Nugget bulges measured from macrographs of weld structure were correlated with the weld parameters of Figure 5. A nugget bulge (δ) in the range of 0.005" to 0.010" correlates with a robust range of processing parameters yielding good strengths and avoiding the precipitous drop in strength.

According to the hypothetical relation between tool design, weld parameters, and nugget bulge in Equation 3 for the same tool geometry nugget bulge is a function of the process

pitch. Equation 3 was used to generate the process parameter range summarized in Figure 8 for the SR-FSWs in this study compared to the effects of using a smaller pin diameter. Currently this relationship doesn't consider the affect of different alloys. It would be expected that lower conductivity alloys would be welded within a different region of the parameter range given in Figure 8 for the same tool geometry.

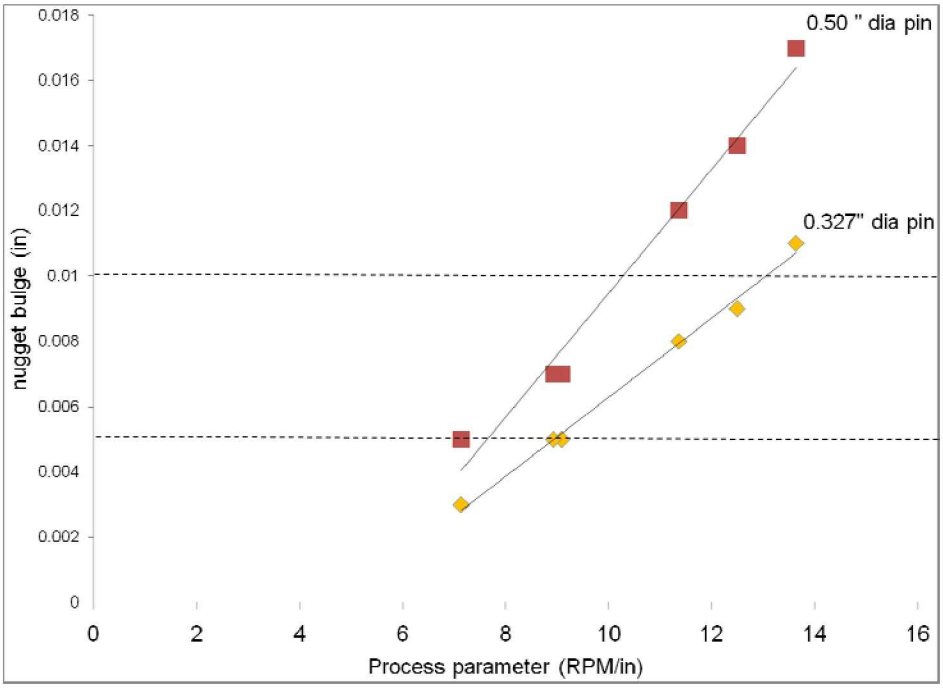

Figure 8. Processing parameter window for constant pitch shoulder and varying pin diameters.

Summary

A correlation between the lateral bulging of the nugget, the grain-refined region in the weld center and the strength of the weld was found in a set of empirical SR-FSW data. Nugget material is generated by the very high shear deformation rate imposed on the weld metal as it is engulfed by and abandoned by the rotating plug of metal adjacent to the tool. The transverse bulge can be explained by a distortion of the nugget caused by the ring vortex flow component. This is in agreement with other observations in which higher RPM resulted in increased nugget area [13]. An approximately for the extent of nugget bulge can be computed in terms of weld parameters and geometric features of the SR-FSW tool.

Because of the correlation of bulge with tensile strength, the bulge computation relates weld parameters and tool geometry to weld strength. This correlation presents a way to select parameters and geometry so as to optimize weld strength. A nominal amount of nugget bulge correlates with a robust operating processing parameter map. As observed, the tensile strength maximizes at the outer edge of this processing map. Thus process parameter selection on the basis of weld strength may not be robust resulting in unacceptable data scatter.

ACKNOWLEDGEMENTS

We wish to acknowledge the EM30 Welding Group at the NASA-MSFC for providing the FSW samples used in this study. One of the authors (MSB) would like to acknowledge the opportunity to participate in this research as part of the 2009 URSP program sponsored by the NASA-MSFC EM 30 welding group. Another author (JAS) would like to acknowledge funding provided by participation in the NASA Intergovernmental Personnel Act.

REFERENCES

1) Thomas, W.M., Nicholas, E.D., Needham, J.C., Murch, M.G., Templesmith, P., Dawes, C.J., Friction Stir Butt Welding, U.S. Patent No. 5,460,317, 1991.

2) Schneider, J.A., Nunes, Jr., A.C., "Characterization of plastic flow and resulting micro textures in a friction stir weld," Met. Trans. B, Vol. 35, p. 777-783, 2004.

3) Schneider, J.A., Beshears, R., Nunes, Jr., A.C., "Interfacial sticking and slipping in the friction stir welding process", *Mat. Sci. & Engr. A*, Vol. 435-436, p. 297-304, 2006.

4) Pew, J.W., Nelson, T.W., Sorensen, C.D., "Development of a Torque-Based Weld Power Model for Friction Stir Welding," *FSW&P IV*, eds. R.S. Mishra, M.W. Mahoney, T.J. Lienert, K.V. Jata, TMS Pub., pp. 73-81, 2007.

5) El-Domiaty, A., El-hafez, H.A., "An Energy Model for Friction Stir Welding," Materials Science and Technology (MS&T) Proceedings, Detroit, MI, pp. 435-447, 2007.

6) Reynolds, A.P., Tang, W., "Alloy, Tool Geometry, and Process Parameter Effects on Friction Stir Weld Energies and Resultant FSW Joint Properties," *FSW&P*, ed. K.V. Jata, M.W. Mahoney, R.S. Mishra, S.L. Semiatin, D.P. Field, TMS Pub., p. 15-23, 2001.

7) Reynolds, A.P., Lindner, K., Tang, W., Seidel, T.U., "Weld efficiency and defect formation: correlation between experiment and simple models," *6th Int'l Trends in Welding Res. Conf. Proc.*, ed. S. A. David, T. DebRoy, J. C. Lippold, H. Smartt, and J. M. Vitek, Pine Mtn., GA, 2003.

8) Arbegast, W.J., "Friction Stir Welding and Processing – Current State of the Art and Needs for the Future," *XXXIII Consolda – Congresso Nacional de Soldagemd*, Caxias do Sul, RS, August 27-30, 2007.

9) Kim, Y.G., Fujii, H., Tsumura, T., Komazaki, T., Nakata, K., "Three defect types in friction stir welding of aluminum die casting alloy," *Mat. Sci. & Engr. A*, Vol. 415, p. 250-254, 2006.

10) Gharacheh, M.A., Kokabi, A.H., Daneshi, G.H., Shalchi, B., Sarrafi, R., "The influence of the ratio of "rotational speed/transverse speed" (ω/v) on mechanical properties of AZ31 friction stir welds," *Int'l J of Machine tools & Mfgt*, Vol. 46, p. 1983-1987, 2006.

11) Colligan, K.J., et. Al., "Friction stir welding of thick section 5083-H131 and 2195-T8P4 aluminum plates," *3rd Int'l FSW Symp.*, Kobe, TWI Pub., Japan, 2001.

12) Record, H.J., et al., "A Look at the Statistical Identification of Critical Process Parameters in Friction Stir Welding," *Welding Journal*, Vol. 86, No. 4, p. 97-s to103-s, 2007.

13) Mishra, R.S., Ma, Z.Y., "Friction stir welding and processing," *Mat. Sci. & Engr. R.*, Vol. 50, p. 1-78, 2005.

14) Charit, I, Mishra, RS, "Abnormal grain growth in friction stir processed alloys," *Scripta Mater.*, Vol. 58, p. 367-371, 2008.

15) Arbegast, W.J., "Modeling Friction Stir Joining as a Metalworking Process," *Hot Deformation of Aluminium Alloys III*, Z. Jin, ed., TMS Pub., 2003.

16) Ren, S.R., Ma., Z.Y., Chen, L.Q., "Effect of welding parameters on tensile properties and fracture behavior of friction stir welded Al-Mg-Si alloy," *Scripta Mater.*, Vol. 56, p. 69-72, 2007.

17) Zettler, R., Lomolino, S., dos Santos, J.F., Donath, T., Beckmann, F., Lippman, T., Lohwasser, D., "Effect of tool geometry and process parameters on material flow in FSW of an AA2024-T351 alloy," *Welding in the world*, Vol. 50, No. 11/12, p. 107-116, 2006.

18) Zhao, Y-H., Lin, S.-B., Wu, L., Qu, F-X., "The influence of pin geometry on bonding and mechanical properties in friction stir weld 2014 Al alloy," *Mat. Letters*, Vol. 59, p. 2948-2952, 2005.

19) Zhao, Y.-H., et al., Influence of pin geometry on material flow in friction stir welding process. *Mat. Sci. & Tech.*, Vol. 22, No. 1, p. 45-50, 2006.

20) Elangovan, K., Balasubramanian, V., "Influences of tool pin profile and tool shoulder diameter on the formation of friction stir processing zone in AA6061 aluminum alloy," *Mat. and Design*, Vol. 29, No. 2, p. 362-373, 2008.

21) Elangovan, K., Balasubramanian, V., "Influences of pin profile and rotational speed of the tool on the formation of friction stir processing zone in AA2219 aluminum alloy", *Mat. Sci. & Engr. A*, Vol. 459, p. 7-18, 2007.

22) Colligan, K.J., Xu, J., Pickens, J.R., "Welding tool and process parameter effects in friction stir welding of aluminum alloys," *FSW&P II*, ed. K.V. Jata, M.W. Mahoney, R.S. Mishra, S.L. Semiatin, and T. Lienert, TSM Pub., p. 181-190, 2003.

23) McClure, J.C., Coronado, E., Aloor, S., Nowak, B.M., Murr, L.E., Nunes, Jr., A.C., "Effect of pin tool shape on metal flow during friction stir welding," *Int'l Conf on Trends in Welding Research Proc.,* ASM Pub., p. 257-261, 2002.

24) Field, D.P., Nelson, T.W, "Tool geometry dependence of local texture in friction stir welds of 7050 aluminum plate," *Mat. Sci. Forum*, Vol., 408-412, p. 1507-1512, 2002.

25) Boz, M., Kurt, A., "The influence of stirrer geometry on bonding and mechanical properties in friction stir welding process," *Mat. & Design*, Vol. 25, p. 343-347, 2004.

26) Fujii, H., Cui, L., Maeda, M., Nogi, K., "Effect of tool shape on mechanical properties and microstructure of friction stir welded aluminum alloys," *Mat. Sci. & Engr. A*, Vol. 419, p. 25-31, 2006.

27) Zhao, Y-H., Lin, S.-B., Wu, L., Qu, F-X., "The influence of pin geometry on bonding and mechanical preoprties in friction stir weld 2014 Al alloy," *Mat. Letters*, Vol. 59, p. 2948-2952, 2005.

28) Lorrain, O., Favier, V., Zahrouni, H., Lawrjaniec, D., "Understanding the material flow path of friction stir welding process using unthreaded tools," *J. Mat. Proc.* Tech., Vol. 210, p. 603-609, 2010.

29) Chen, Z.W., Pasang, T., Qi, Y., "Shear flow and formation of nugget zone during friction stir welding of aluminum alloy 5083-0," *Mat. Sci. & Engr. A*, Vol. 474, p. 312-316, 2008.

30) Kumar, K., Kailas, S.V., "The role of friction stir welding tool on material flow and weld formation," *Mat. Sci. & Engr. A*, Vol. 485, p. 367-374, 2008.

31) Scialpi, A., DeFilippis, L.A.C., Cavaliere, P., "Influence of shoulder geometry on microstructure and mechanical properties of friction stir welded 6082 aluminum alloys," *Mat. & Design*, Vol. 28, p. 1124-1129, 2007.

32) Leal, R.M., Leitao, C., Loureiro, A., Rodriques, D.M., Vilaca, P., "Material flow in heterogeneous friction stir welding of thin aluminum sheets: effect of shoulder geometry," *Mat. Sci. & Engr. A.*, Vol 498, p. 384-391, 2008.

33) Yan, D.P., "Study of shoulder flow zone formation in thick section FSW of 6061 Al alloy using scroll shoulder tool," *MPhil Thesis*, Auckland University of Technology, 2008.

34) Czochralski, J., "Zunahme der Keimzahl mit Steingender Temperatur", *Moderne Metallkunde*, 1924.

35) Kaibyshev, R., Mazurina, I., "Mechanisms of grain refinement in aluminum alloys during severe plastic deformation," *Mat. Sci. Forum*, Vol. 467-470, p. 1251-1260, 2004.

36) Brick, R.M, Gordon, R.B., Phillips, A., Structure and Properties of Alloys: The application of phase diagrams to the interpretation and control of industrial alloy structures, 3rd ed., pub. McGraw Hill, p. 161, 1965.

37) London, B., Mahoney, M., Bingel, W., Calabrese, M., Bossi, R.H., Waldron, D., *FSW&P II*, eds. K.V. Jata, M.W. Mahoney, R.S. Mishra, S.L. Semiatin, T. Lienert, TMS Pub., p. 3-12, 2003.

38) ASTM Standard E8, "Standard Test Methods for Tension Testing of Metallic Materials," ASTM International, West Conshohocken, PA, Vol. 3.01.